J Incl Phenom Macrocycl Chem (2010) 68:313–322
DOI 10.1007/s10847-010-9790-8

ORIGINAL ARTICLE

Inclusion complexes of cyclodextrins with 4-amino-1,8-naphthalimides (part 2)

Barbara Perez Gonçalves Silva · Rodrigo Oliveira Marcon · Sergio Brochsztain

Received: 2 February 2010 / Accepted: 15 April 2010 / Published online: 7 May 2010

Abstract Fluorescence spectroscopy was used to characterize inclusion compounds between 4-amino-1,8-naphthalimides (ANI) derivatives and different cyclodextrins (CDs). The ANI derivatives employed were *N*-(12-aminododecyl)-4-amino-1,8-naphthalimide (*mono*-C_{12}ANI) and *N,N'*-(1,12-dodecanediyl)bis-4-amino-1,8-naphthalimide (*bis*-C_{12}ANI). The CDs used here were α-CD, β-CD, γ-CD, HP-α-CD, HP-β-CD and HP-γ-CD. The presence of CDs resulted in pronounced blue-shifts in the emission spectra of the ANI derivatives, with increases in emission intensity. This behavior was parallel to that observed for the dyes in apolar solvents, indicating that inclusion complexes were formed between the ANI and the CDs. *Mono*-C_{12}ANI formed inclusion complexes of 1:1 stoichiometry with all the CDs studied. Complexes with the larger CDs (HP-β-CD, HP-γ-CD and γ-CD) were formed by inclusion of the chromophoric ANI ring system, whereas the smaller CDs (α-CD, HP-α-CD and β-CD) formed complexes with *mono*-C_{12}ANI by inclusion of the dodecyl chain. *Bis*-C_{12}ANI formed inclusion complexes of 1:2 stoichiometry with HP-β-CD, HP-γ-CD and γ-CD, but did not form inclusion complexes with α-CD, HP-α-CD and β-CD. The data were treated in the case of the large CDs using a Benesi-Hildebrand like equation, giving the following equilibrium constants: *mono*-C_{12}ANI:HP-β-CD ($K_{11} = 50\ M^{-1}$), *mono*-C_{12}ANI:HP-γ-CD ($K_{11} = 180\ M^{-1}$), *bis*-C_{12}ANI:HP-β-CD ($K_{12} = 146\ M^{-2}$), *bis*-C_{12}ANI:HP-γ-CD ($K_{12} = 280\ M^{-2}$).

Keywords 4-amino-1,8-naphthalimides · Cyclodextrins · Inclusion complexes · Fluorescent dyes

Electronic supplementary material The online version of this article (doi:10.1007/s10847-010-9790-8) contains supplementary material, which is available to authorized users.

B. P. G. Silva · S. Brochsztain (✉)
Universidade Federal do ABC, Rua Santa Adélia, 166, Santo André, SP 09210-170, Brazil
e-mail: sergio.brochsztain@ufabc.edu.br

R. O. Marcon
Centro Interdisciplinar de Investigação Bioquímica, Universidade de Mogi das Cruzes, Av. Dr. Cândido Xavier de Almeida Souza, 200, Mogi das Cruzes, SP 08780-911, Brazil

Introduction

The 4-amino-1,8-naphthalimides (ANI) constitute a class of highly fluorescent organic dyes [1–6], which are soluble both in water and in organic solvents. Thank to their outstanding photophysical properties, the ANI have been used in several applications, such as fluorescent sensors for cations [7–9] and anions [10, 11], molecular switches [12, 13], systems for the harvesting of solar energy [14–16] and thermochromic [17] and pH sensing [18] devices, among others. The ANI are also useful as building blocks for the construction of supramolecular systems, such as rotaxanes and catenanes [19, 20]. Recently, the properties of the ANI as nucleic acids intercalators have been explored for the binding and photochemical cleavage of DNA [21–23], making the ANI potential candidates as antitumor agents. Other biological applications for the ANI include fluorescent labeling agents for biological cells [24–26], antiviral agents [27, 28] and in the promotion of photochemical protein crosslinking [29].

Considering the wide range of applications available for the ANI derivatives, it is of great interest to study the inclusion complexes of these dyes with cyclodextrins (CDs). The CDs are cyclic oligossacharides that form inclusion complexes with a great variety of organic compounds in aqueous solution [30–33]. Inclusion of the ANI in the hydrophobic CD cavity is expected to change the photophysical properties of the dyes, increasing the scope of their use as sensors, switches or solar energy collectors. Regarding medical applications, the CDs are well known to increase water solubility of included drugs, thus improving the bioavailability and altering tissue distribution of the ANI. Complexes between ANI and cyclodextrins can also be explored as starting materials for the synthesis of cyclodextrin-based rotaxanes and catenanes [34].

Our group has studied the inclusion of different aromatic imides and diimides in the cavity of cyclodextrins [35–37]. In a previous article, we showed that phosphonate-substituted ANI derivatives form complexes with several CDs [37], leading to increased fluorescence intensities. In the present work, we continue our studies with two new ANI derivatives synthesized by our group: *N*-(12-aminododecyl)-4-amino-1,8-naphthalimide (*mono*-C_{12}ANI) and *N,N′*-(1,12-dodecanediyl)bis-4-amino-1,8-naphthalimide (*bis*-C_{12}ANI), whose structures are shown in Scheme 1.

Experimental part

Materials

All solvents used for fluorescent measurements were spectroscopic grade (Merck or J.T. Baker). Imidazole was purchased from Merck. Aqueous solutions were prepared with deionized water. Buffer solutions were prepared with high purity salts. The following reagents were purchased from Aldrich: 4-amino-1,8-naphthalic anhydride, 1,12-diaminododecane, α-cyclodextrin (α-CD), β-cyclodextrin (β-CD), γ-cyclodextrin (γ-CD), 2-hydroxypropyl-α-cyclodextrin (HP-α-CD) (molar substitution = 0.6, MW ≈ 1,180), 2-hydroxypropyl-β-cyclodextrin (HP-β-CD) (molar substitution = 0.6, MW ≈ 1,380), 2-hydroxypropyl-γ-cyclodextrin (HP-γ-CD) (molar substitution = 0.6, MW ≈ 1,580), quinine sulfate dihydrate, tetrabutylammonium tetrafluoroborate.

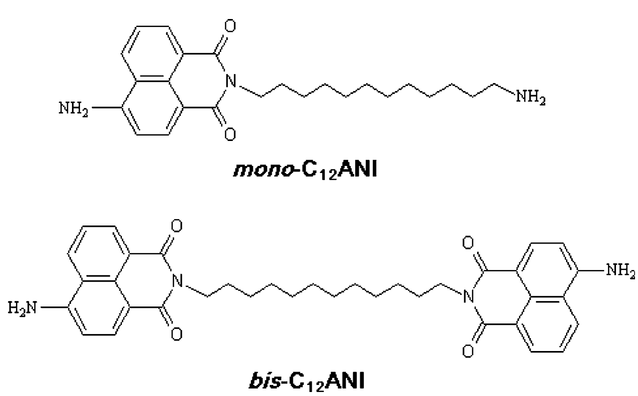

Scheme 1 Structures of the ANI derivatives employed in this work

Synthesis of *mono*-C_{12}ANI and *bis*-C_{12}ANI

The ANI derivatives were synthesized using molten imidazole as a solvent. Imidazole is an excellent solvent for the synthesis of aromatic imides [38, 39] because it dissolves the precursors (anhydrides and primary amines), which are otherwise insoluble in most common solvents.

N-(12-aminododecyl)-4-amino-1,8-naphthalimide (*mono*-C_{12}ANI): A mixture of 4-amino-1,8-naphthalic anhydride (100 mg, 0.47 mmol), 1,12-diaminododecane (188 mg, 0.94 mmol) and imidazole (0.5 g) was heated at 120-140 °C for 1 h. After cooling, 10 mL of acetonitrile were added, and the resulting precipitate was filtered off, washed with cold acetonitrile and dried. The crude product was then purified by chromatography in silica gel, using a gradient of chloroform/ethanol as the eluent, giving 91 mg of *mono*-C_{12}ANI (49% yield). Melting point >400 °C. Elemental analysis (CHN), obtained (calculated): 57.3% C (73.1%); 7.87% H (8.12%); 10.2% N (10.7%). A lower than expected carbon content has been found for several aromatic imides, and has been attributed to incomplete combustion [40]. However, since traces of impurities (mainly 1,12-diaminododecane and *bis*-C_{12}ANI) were found in the ^{1}H-NMR spectra of *mono*-C_{12}ANI, even after chromatography, an analytically pure sample for the experiments with CDs was obtained by HPLC (see Supplementary Material).

N,N′-(1,12-dodecanediyl)bis-4-amino-1,8-naphthalimide (*bis*-C_{12}ANI): A mixture of 4-amino-1,8-naphthalic anhydride (300 mg, 1.41 mmol), 1,12-diaminododecane (141 mg, 0.71 mmol) and imidazole (1.5 g) was heated at 120-140 °C for 1 h. After cooling, 10 mL of ethanol were added, and the resulting precipitate was filtered off, washed with cold ethanol and dried. The crude product was then purified by recrystallization with 1,2-dichloroethane, giving 164 mg of *bis*-C_{12}ANI (39% yield). Melting point >400 °C. Elemental analysis (CHN), obtained (calculated): 70.2% C (73.2%); 6.23% H (6.44%); 9.03% N (9.49%). ^{1}H-NMR and HPLC: see Supplementary Material.

Methods

Fluorescence measurements were performed with a Hitachi F-2500 fluorescence spectrophotometer. Aqueous solutions with varying concentrations of CDs for binding studies were prepared as follows: concentrated stock solutions (0.01–0.1 M) of the CDs were prepared in aqueous buffer solutions. Aliquots from these stock solutions were then mixed with aliquots from the buffer in test tubes to give the desired CD concentration (total volume of 2.0 mL). Aliquots from the ANI derivatives (2 μL from 1 mM stock solutions in *N,N*-dimethylformamide) were then added to each tube, giving [ANI] = 1.0×10^{-6} M. The tubes were mixed in a shaker for 24 h at 25 °C for equilibration before measuring the fluorescence spectra.

Cyclic voltammetry was performed using an Autolab PGSTAT-30 Potentiostat/Galvanostat. The measurements were carried out at room temperature (25 ± 1 °C) in a three-compartment electrochemical cell with a carbon working electrode, a platinum auxiliary electrode and a saturated Ag/AgCl reference electrode in 3 M KCl. *N,N*-dimethylformamide (DMF) was used as a solvent, containing 0.01 M tetrabutylammonium tetrafluoroborate as a support electrolyte. Solutions were degassed with argon for 5 min prior to measurements.

Results and discussion

Characterization of ANI derivatives in solution

The absorption and emission spectra of *mono*-C_{12}ANI and *bis*-C_{12}ANI were quite sensitive to solvent polarity. The absorption maximum of *bis*-C_{12}ANI, for instance, was red-shifted from 408 nm in chloroform to 435 nm in water, whereas the emission maximum varied from 501 nm in chloroform to 550 nm in water. Considering that the changes in the emission spectra were by far more pronounced then those observed in the absorption spectra, fluorescence measurements were employed in the present study.

Figure 1 and Table 1 show the solvent effects on the emission spectra of *mono*-C_{12}ANI and *bis*-C_{12}ANI. The emission maximum of *mono*-C_{12}ANI was red-shifted from 510 nm in chloroform to 520 nm in ethanol and 535 nm in water. In the case of *bis*-C_{12}ANI, the emission maximum was 501 nm in chloroform, 519 nm in ethanol and 550 nm in water. The emission spectra in water were identical, for both *mono*-C_{12}ANI and *bis*-C_{12}ANI, when registered at pH 4.5, 6.0 and 8.5 (Table 1), indicating that the spectral properties were insensitive to the protonation state of the amino groups.

The pronounced solvent effects on the spectra of ANI derivatives has been attributed to the charge-transfer character of the $S_0 \rightarrow S_1$ transition [14, 15], from a neutral ground-state to a charge-separated excited-state (Scheme 2). Since in polar solvents the charged excited-state is more stabilized by solvation than the neutral ground-state, the transition energy decreases, resulting in the observed red-shift with increasing polarity.

The solvent effects on the emission of *bis*-C_{12}ANI were more pronounced than in the case of *mono*-C_{12}ANI (Fig. 1, Table 1). A red-shift of nearly 50 nm was observed for *bis*-C_{12}ANI as going from $CHCl_3$ to H_2O, as compared to the

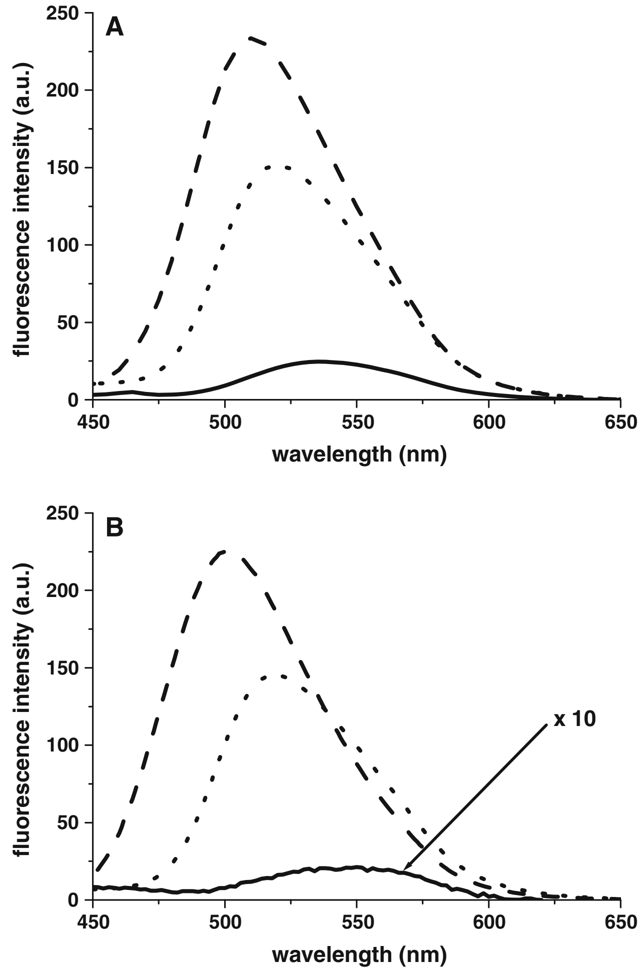

Fig. 1 Emission spectra ($\lambda_{ex} = 375$ nm) of *mono*-C_{12}ANI (**a**) and *bis*-C_{12}ANI (**b**) in solvents of different polarities: chloroform (- - -), ethanol (···) and water (buffered at pH 6.0) (—). The dye concentration was 1×10^{-6} M in all cases

Table 1 Fluorescence data ($\lambda_{ex} = 375$ nm) for *mono*-C_{12}ANI and *bis*-C_{12}ANI in different solvents

Solvent	*mono*-C_{12}ANI		*bis*-C_{12}ANI	
	λ_{max} (nm)	$\phi_f^{a,b}$	λ_{max} (nm)	$\phi_f^{a,b}$
$CHCl_3$	510	0.26	501	0.24
CH_3CN	510	0.25	508	0.19
DMF	515	0.16	515	0.24
EtOH	520	0.17	519	0.16
H_2O (pH 4.5)	535	0.049	550	0.0022
H_2O (pH 6.0)	535	0.036	550	0.0023
H_2O (pH 8.5)	535	0.036	550	0.0023

The dye concentration was 1×10^{-6} M in both cases

[a] Fluorescence quantum yield (reference: 1 mM quinine sulfate in 0.5 M H_2SO_4)

[b] The error in the quantum yield measurement is ±5% of the given value

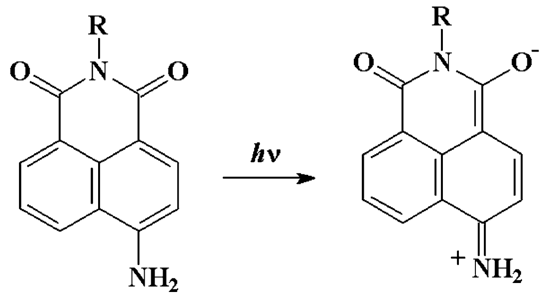

Scheme 2 Charge-transfer $S_0 \rightarrow S_1$ transition for ANI derivatives, from a neutral ground-state to a charge-separated excited state

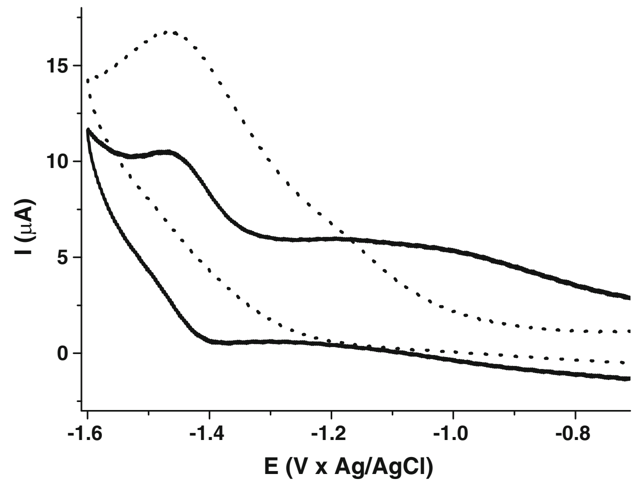

Fig. 2 Cyclic voltammograms of *mono*-C_{12}ANI (···) and *bis*-C_{12}ANI (—) in DMF containing 0.01 M tetrabutylammonium tetrafluoroborate. Scan rate: 200 mV/s

25 nm shift in the case of *mono*-C_{12}ANI. Moreover, the emission maximum of *bis*-C_{12}ANI in water was 15 nm red-shifted as compared to that of *mono*-C_{12}ANI. It can also be noticed in Fig. 1 that the fluorescence of *bis*-C_{12}ANI in water was quenched relative to that of *mono*-C_{12}ANI, with a decrease of an order of magnitude in the quantum yield (Table 1). The behavior of *bis*-C_{12}ANI in water suggests that the excited molecule folds about the dodecyl link to form an intramolecular excimer between the two ANI units (see Scheme 3), resulting in the observed red-shift and fluorescence quenching, in a process which is not possible in the case of *mono*-C_{12}ANI.

Electrochemical data on the two ANI derivatives in DMF are presented in Fig. 2 and Table 2. It is known [2] that ANI derivatives can be either oxidized (at the amino group) or reduced (at the imide group), as can be deduced from the charge-separated excited state in Scheme 2. Both *mono*-C_{12}ANI and *bis*-C_{12}ANI display two reversible oxidations waves near 1.0 and 1.5 V (Table 2), in agreement with literature data [2]. When the cyclic voltammograms were recorded in the negative direction (Fig. 2), *mono*-C_{12}ANI displayed only one reduction wave at −1.36 V, corresponding to anion radical formation, as reported in the literature [2]. In the case of *bis*-C_{12}ANI, however, the reduction occurred in two steps, resulting in two waves with lower current at −1.17 and −1.43 V.

These results show that the two ANI units in *bis*-C_{12}ANI are not reduced at once, but stepwise, suggesting a stabilizing interaction between the ANI units. If there was no interaction between the two imide rings, they would be reduced at once and a two-electron one wave reduction would be observed (Scheme 3). Since the dodecyl chain linking the two ANI units does not allow through-bond conjugation, it can be presumed that *bis*-C_{12}ANI folds about the alkyl chain upon reduction of one of the rings, giving a stabilized intramolecular dimer (Scheme 3), pairing an ANI anion radical with an unreduced ANI ring ($ANI/ANI^{-\cdot}$). This explanation corroborates the formation of the intramolecular excimer suggested above.

Studies of complex formation between ANI derivatives and cyclodextrins

The high solvent sensitivity of the emission spectra of ANI derivatives is very convenient to study the inclusion of these dyes in the cavity of cyclodextrins. It is well known

Scheme 3 **a** Two step reduction of *bis*-C_{12}ANI, with stabilization of the $ANI/ANI^{-\cdot}$ pair. **b** One step reduction of *bis*-C_{12}ANI, which would be expected if there was no ring-ring interaction

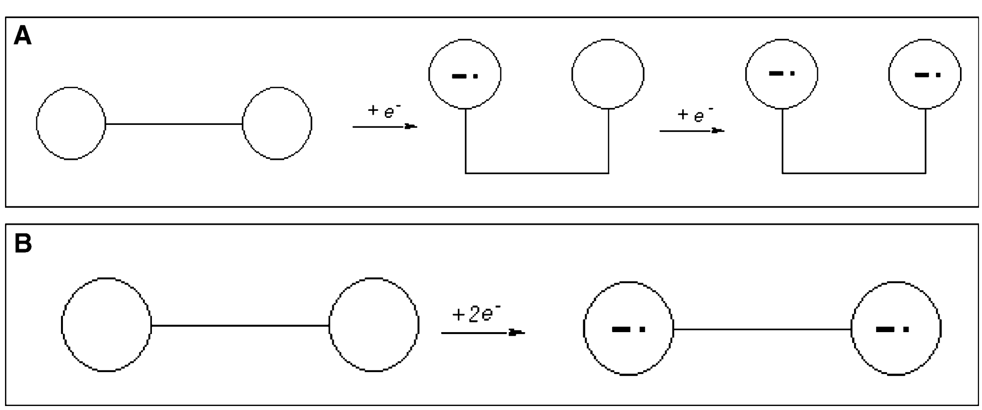

Table 2 Half-wave potentials (V × Ag/AgCl) for the oxidation and reduction of 1 mM *mono*-C_{12}ANI and *bis*-C_{12}ANI in DMF containing 0.01 M tetrabutylammonium tetrafluoroborate

	Oxidation		Reduction	
mono-C_{12}ANI	1.47	1.02	−1.36	–
bis-C_{12}ANI	1.50	1.02	−1.17	−1.43

that the polarity inside the cavity of CDs is similar to ethanol solution. Therefore, the formation of host–guest complexes should result in the transfer of the dye from bulk water to a less polar environment, what expectedly (see Fig. 1) would cause an increase in the fluorescence intensity and a blue shift.

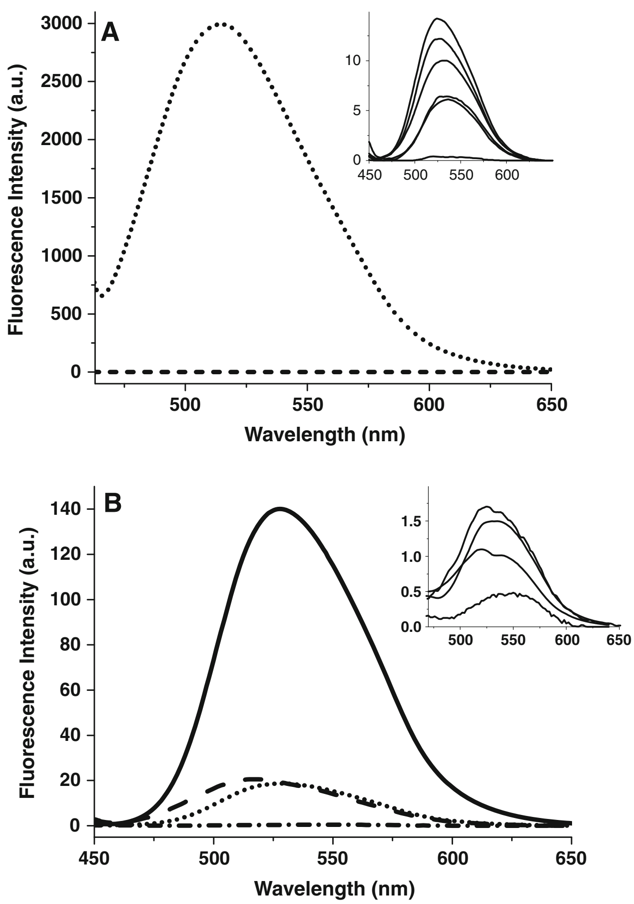

Fig. 3 Effect of cyclodextrins on the emission spectra of ANI derivatives ($\lambda_{ex} = 440$ nm). **a** *Mono*-C_{12}ANI in water (- - -) and in the presence of 0.03 M γ-CD (···). Inset (from bottom to top): *mono*-C_{12}ANI in water and in the presence of 0.01 M β-CD, 0.05 M α-CD, 0.1 M HP-α-CD, 0.1 M HP-γ-CD and 0.1 M HP-β-CD. (**b**) *Bis*-C_{12}ANI in water (-·-·-) and in the presence of 0.03 M γ-CD (- - -), 0.1 M HP-γ-CD (···) and 0.1 M HP-β-CD (—). Inset (from bottom to top): *bis*-C_{12}ANI in water and in the presence of 0.05 M α-CD, 0.01 M β-CD and 0.1 M HP-α-CD. The dye concentration was 1×10^{-6} M in all cases

The effects of the presence of different cyclodextrins on the emission spectra of *mono*-C_{12}ANI and *bis*-C_{12}ANI are shown in Fig. 3 and Table 3. In the case of *bis*-C_{12}ANI, the presence of γ-CD, HP-γ-CD and HP-β-CD resulted in pronounced blue shifts ($\Delta\lambda = 33$, 21 and 22 nm, respectively) and increased fluorescence intensities ($I_{CD}/I_{water} = 40$, 38 and 280, respectively), indicating the formation of inclusion complexes, thus hindering the formation of the intramolecular excimer observed in water. In the case of the other CDs (α-CD, HP-α-CD and β-CD), however, smaller effects were observed (12–14 nm blue shifts and two to threefold increases in emission intensity). Taking into account geometrical considerations (Scheme 4b), these effects are most likely due to external interactions (such as hydrogen bonding), rather than true inclusion effects.

The binding sites for the CDs in *bis*-C_{12}ANI are the two bulky aromatic imide rings at the ends of the molecule, as shown in Scheme 4b. Therefore, only CDs with a large cavity (γ-CD, HP-γ-CD and HP-β-CD) could complex with *bis*-C_{12}ANI, which is in full agreement with the results in Fig. 3 and Table 3. Although in principle the smaller CDs (α-CD, HP-α-CD and β-CD) could host the alkyl chain linking the two imide rings, forming a pseudo-rotaxane, they are too small to slip through the ANI ring system (Scheme 4b). According to Scheme 4b, it is expected that the large CDs form complexes with 1:2 stoichiometry (ANI:CD_2) with *bis*-C_{12}ANI, what was confirmed by the upward curvature observed in the binding isotherms (Fig. 4b, see below).

Table 3 Fluorescence data for *mono*-C_{12}ANI and *bis*-C_{12}ANI in the presence of different cyclodextrins

Solution[a]	*mono*-C_{12}ANI			*bis*-C_{12}ANI		
	λ_{max} (nm)	I_{sol}/I_W[b]	Complex	λ_{max} (nm)	I_{sol}/I_W[b]	Complex
H_2O	535	–	–	550	–	–
0.05 M α-CD	536	18	Yes	538	2	No
0.01 M β-CD	536	17	Yes	536	3	No
0.03 M γ-CD	515	8300	Yes	517	40	Yes
0.1 M HP-α-CD	532	28	Yes	538	3	No
0.1 M HP-β-CD	524	39	Yes	528	280	Yes
0.1 M HP-γ-CD	528	34	Yes	529	38	Yes
EtOH	520	5	–	519	74	–

Data in water and ethanol are included for comparison. The dye concentration was 1×10^{-6} M in both cases

[a] Aqueous solutions were prepared in 0.01 M phosphate buffer (pH 7.0)

[b] Ratio between the fluorescence intensity (measured at λ_{max}) in the given solution and in water

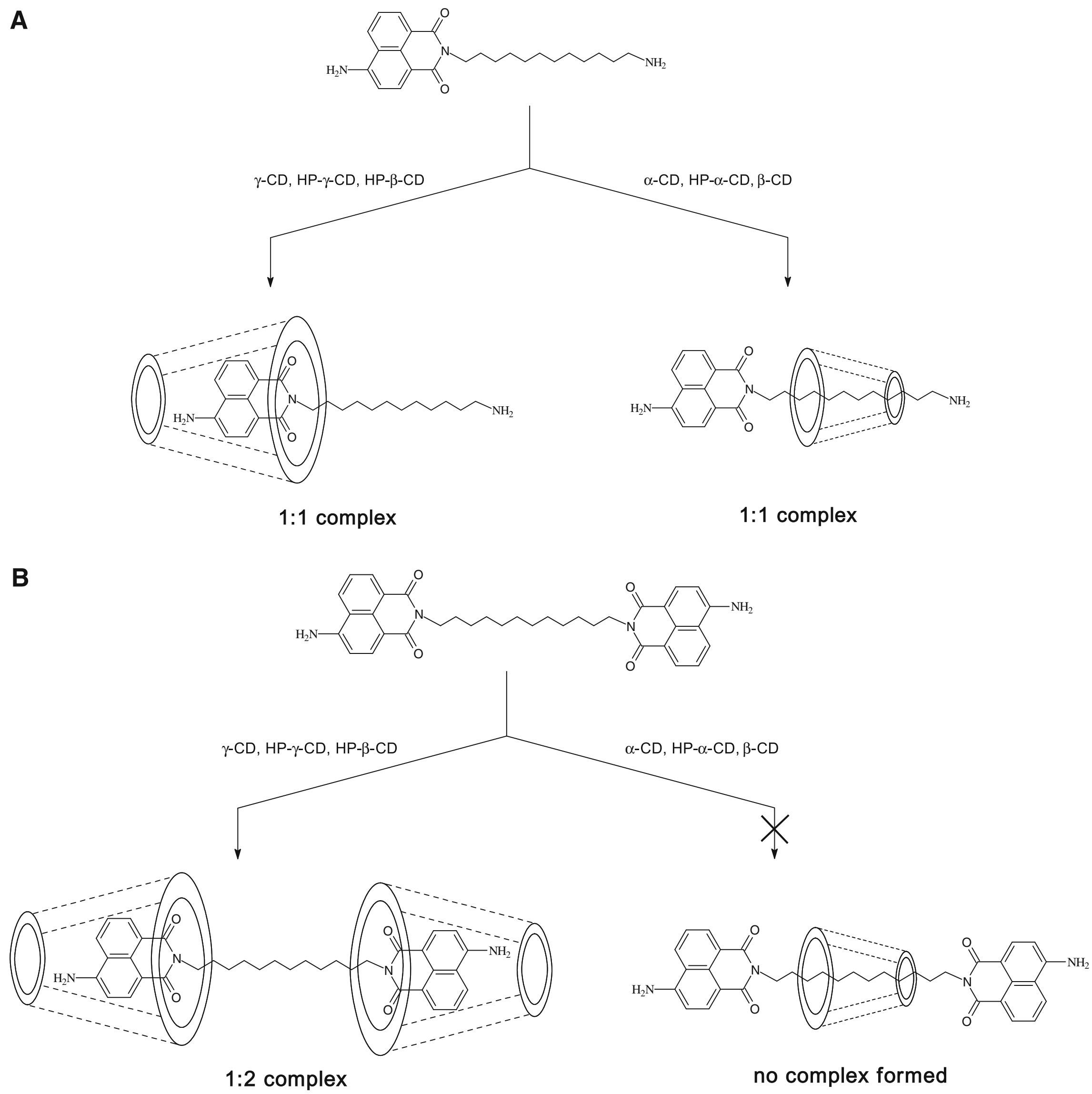

Scheme 4 Suggested complexation modes for the interaction between different cyclodextrins and *mono*-C_{12}ANI (**a**) and *bis*-C_{12}ANI (**b**)

In the case of *mono*-C_{12}ANI, the effect of the CDs shown in Fig. 3 and Table 3 suggest complex formation with all the CDs studied, as expected, since this compound has two binding sites of different geometry available (Scheme 4a), one for the large CDs (the imide ring) and the other for the smaller CDs (the alkyl chain). The effects observed with α-CD, HP-α-CD and *β*-CD were smaller than those observed with the large CDs, as expected, since the chromophoric portion of the molecule is the imide ring, rather than the alkyl chain. Complexes of CDs with *mono*-C_{12}ANI are expected to have a 1:1 stoichiometry (Scheme 4a), what was confirmed by the downward curvature of the binding isotherms (Fig. 4a, see below).

It is remarkable the large blue shift shown by both *mono*-C_{12}ANI and *bis*-C_{12}ANI in the presence of *γ*-CD. The emission maxima of the *γ*-CD complexes (λ_{max} = 515–517 nm) is even shorter than the maxima in ethanol solution (λ_{max} = 519–520 nm, Table 1), showing that the chromophoric imide group was included deeply inside the *γ*-CD cavity, in contact with the hydrophobic ring core. Less pronounced blue shifts were noticed with HP-*β*-CD and HP-*γ*-CD (λ_{max} = 524–529 nm), suggesting a more external inclusion mode, probably involving the extended part of the cavity provided by the flexible hydroxypropyl chains, which can also make multiple hydrogen bonds with the dyes. Another evidence for this is the fact that HP-*β*-CD forms complexes with *bis*-C_{12}ANI, whereas *β*-CD does not (Table 3), what proves that the ANI group does not fit inside the *β*-CD cavity without the extending HP chains.

Binding isotherms

A more detailed picture of the inclusion process can be gained by performing binding isotherms. For this purpose, we used HP-β-CD, γ-CD and HP-γ-CD, since these are the CDs that caused the largest effects in the experiments above. The effects of increasing concentration of HP-β-CD on the emission spectra of *mono*-C_{12}ANI and *bis*-C_{12}ANI are shown in Fig. 4. The other CDs studied, γ-CD and HP-γ-CD, displayed similar behavior (inset of Fig. 4 and Supplementary Material). A rather distinct behavior can be noticed when comparing the two compounds. For *mono*-C_{12}ANI, the initial additions of CD caused large fluorescence increases, but at high CD concentrations the emission intensity tends to saturate, generating binding isotherms with a downward curvature (Fig. 4a). This behavior is typical of the formation of complexes with 1:1 stoichiometry [41, 42], as shown in Scheme 4a. In the case of *bis*-C_{12}ANI, however, the opposite behavior was observed. Initial additions of CD caused very small changes, but at higher CD concentrations the emission intensity starts increasing rapidly, generating isotherms with an upward curvature (Fig. 4b), indicating the formation of complexes with more than one CD per host molecule (presumably 1:2, according to geometrical considerations, see Scheme 4b).

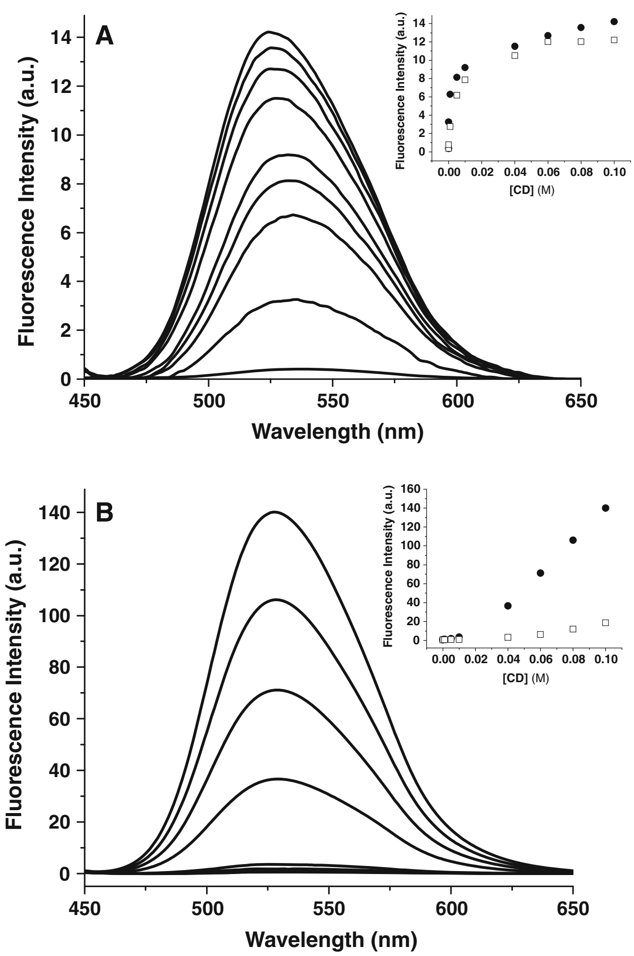

Fig. 4 Effect of increasing concentrations of HP-β-CD on the emission spectra ($\lambda_{ex} = 440$ nm) of *mono*-C_{12}ANI (**a**) and *bis*-C_{12}ANI (**b**). The [HP-β-CD] (M) employed for both experiments are as follows (from bottom to top): 0, 1×10^{-4}, 1×10^{-3}, 5×10^{-3}, 0.01, 0.04, 0.06, 0.08 and 0.1. The dye concentration was 1×10^{-6} M in both cases. Inset: fluorescence intensity as a function of CD concentration (binding isotherms) for *mono*-C_{12}ANI (**a**) and *bis*-C_{12}ANI (**b**) with HP-β-CD (●) and HP-γ-CD (□)

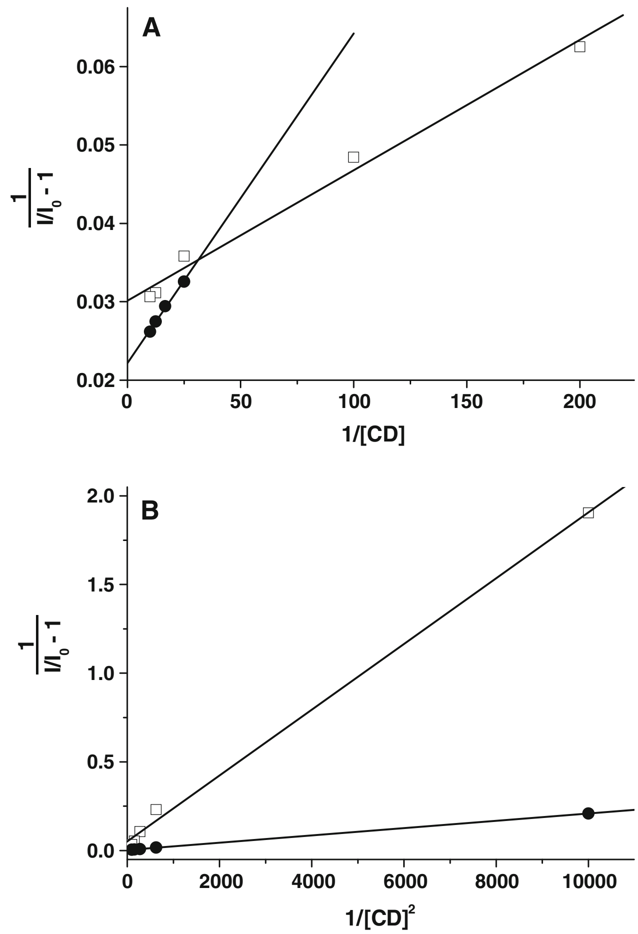

Fig. 5 **a** Benesi-Hildebrand like plots according with Eq. 3 for the 1:1 binding isotherms of *mono*-C_{12}ANI with HP-β-CD (●) and HP-γ-CD (□). **b** Plots according with Eq. 6 for the 1:2 binding isotherms of *bis*-C_{12}ANI with HP-β-CD (●) and HP-γ-CD (□)

In the simple case of 1:1 stoichiometry, the equilibrium represented by Eq. 1 is related to the equilibrium constant K_{11}, as shown in Eq. 2. For this case, the fluorescence data can be treated according to Eq. 3, which has been used by our group [35–37] and others [41–43] for 1:1 binding isotherms between cyclodextrins and fluorescent dyes. In Eq. 3, I_0 and I represent the fluorescence intensities in the absence and in the presence of a given CD, whereas ϕ_0 and

ϕ are the corresponding quantum yields. According to Eq. 3, a plot of $\frac{1}{(I/I_0-1)}$ against the reciprocal of the CD concentration should give a straight line, and the equilibrium constant K_{11} can be obtained by dividing the intercept by the slope (this treatment is a variation of the Benesi-Hildebrand approach).

$$\mathrm{ANI} + \mathrm{CD} \rightleftharpoons \mathrm{ANI} - \mathrm{CD} \quad (1)$$

$$K_{11} = \frac{[\mathrm{ANI} - \mathrm{CD}]}{[\mathrm{ANI}][\mathrm{CD}]} \quad (2)$$

$$\frac{1}{(I/I_0 - 1)} = \frac{1}{(\phi_{\mathrm{CD}}/\phi_0 - 1)} + \frac{1}{(\phi_{\mathrm{CD}}/\phi_0 - 1)K_{11}} \frac{1}{[\mathrm{CD}]} \quad (3)$$

The isotherms for the binding of *mono*-C_{12}ANI with cyclodextrins were then treated according to Eq. 3 (Fig. 5a). Reasonable linear fits were obtained using the points with higher CD concentrations (for low concentrations the fluorescence is weak and hence subject to noise variations). The equilibrium constants (K_{11}) obtained for *mono*-C_{12}ANI from the plots in Fig. 5 are 50 M^{-1} for the complex with HP-β-CD and 180 M^{-1} for the complex with HP-γ-CD (Table 4). These equilibrium constants are of the same magnitude as found for other ANI derivatives with the same CDs in our previous report [37].

In the case of *bis*-C_{12}ANI, geometric considerations (Scheme 4), together with the experimental data (Fig. 4), suggest a 1:2 stoichiometry. In this case, Eqs. 1–3 should be replaced by Eqs. 4–6 [41, 42]. According to Eq. 6, a plot of $\frac{1}{(I/I_0-1)}$ against $\frac{1}{[\mathrm{CD}]^2}$ should give a straight line, and the equilibrium constant K_{12} can be obtained by dividing the intercept by the slope, in analogy to the treatment given above for 1:1 complexes. The results of the treatment for *bis*-C_{12}ANI according to Eq. 6 are presented in Fig. 5b. Reasonable linear fits were obtained, giving equilibrium constants (K_{12}) of 146 M^{-2} for the complex with HP-β-CD and 280 M^{-2} for the complex with HP-γ-CD (Table 4).

$$\mathrm{ANI} + 2\mathrm{CD} \rightleftharpoons \mathrm{ANI} - \mathrm{CD}_2 \quad (4)$$

$$K_{12} = \frac{[\mathrm{ANI} - \mathrm{CD}_2]}{[\mathrm{ANI}][\mathrm{CD}]^2} \quad (5)$$

$$\frac{1}{(I/I_0 - 1)} = \frac{1}{(\phi_{\mathrm{CD}}/\phi_0 - 1)} + \frac{1}{(\phi_{\mathrm{CD}}/\phi_0 - 1)K_{12}} \frac{1}{[\mathrm{CD}]^2} \quad (6)$$

Data for complex formation between the ANI derivatives and γ-CD are given as Supplementary Material. The isotherms show a complex behavior in this case and are not linear with Eqs. 3 or 6, although the downward curvature of the isotherm for *mono*-C_{12}ANI and the upward curvature for *bis*-C_{12}ANI were also observed, as in the case of the other CDs studied. We are presently performing more detailed studies with the ANI derivatives in the presence of γ-CD.

Table 4 Equilibrium constants and stoichiometries obtained for the complexes between ANI derivatives and cyclodextrins

Compound	CD	Stoichiometry	K_{eq}
mono-C_{12}ANI	HP-β-CD	1:1	50 M^{-1}
	HP-γ-CD	1:1	180 M^{-1}
	γ-CD	1:1	Non-linear
bis-C_{12}ANI	HP-β-CD	1:2	146 M^{-2}
	HP-γ-CD	1:2	280 M^{-2}
	γ-CD	1:2	Non-linear

Conclusions

The fluorescence spectra of the ANI derivatives studied here were very sensitive to inclusion in the CD cavity, showing pronounced blue-shifts and increases in the emission intensity upon complex formation. *Mono*-C_{12}ANI was shown to form inclusion complexes of 1:1 stoichiometry with all the CDs studied, but complexes with the larger CDs (HP-β-CD, HP-γ-CD and γ-CD) caused large spectral changes, suggesting the inclusion of the chromophoric group (the ANI ring system). With the smaller CDs (α-CD, HP-α-CD and β-CD), *mono*-C_{12}ANI forms complexes by inclusion of the dodecyl chain, since the ANI ring is too large to fit inside their cavities. *Bis*-C_{12}ANI forms complexes of 1:2 stoichiometry with HP-β-CD, HP-γ-CD and γ-CD, since there are two binding sites (the ANI rings) per molecule. However, *bis*-C_{12}ANI does not form complexes with α-CD, HP-α-CD and β-CD, since they can not slip through the ANI rings to be accommodated around the dodecyl chain. The ANI-CD complexes studied here are quite interesting for biological and medical applications, as well as intermediates in the synthesis of rotaxanes.

Acknowledgments This work was supported by grants from Brazilian agency FAPESP (grant No. 05/51104-4 and 08/57940-7). S.B. thanks CNPq for a PQ scholarship. B.P.G.S. and R.O.M. are grateful to FAPESP for doctoral fellowships.

References

1. Alexiou, M.S., Tychopoulos, V., Ghorbanian, S., Tyman, J.H.P., Brown, R.G., Brittain, P.I.: The UV–visible absorption and fluorescence of some substituted 1,8-naphthalimides and naphthalic anhydrides. J. Chem. Soc. Perkin Trans. **2**, 837–842 (1990)
2. Saha, S., Samanta, A.: Influence of the structure of the amino group and polarity of the medium on the photophysical behavior of 4-amino-1,8-naphthalimide derivatives. J. Phys. Chem. A **106**, 4763–4771 (2002)

3. Prezhdo, O.V., Uspenskii, B.V., Prezhdo, V.V., Boszczyk, W., Distanov, V.B.: Synthesis and spectral-luminescent characteristics of *N*-substituted 1,8-naphthalimides. Dyes Pigments **72**, 42–46 (2007)
4. Qian, J., Xu, Y., Qian, X., Wang, J., Zhang, S.: Effects of anionic surfactant SDS on the photophysical properties of two fluorescent molecular sensors. J. Photochem. Photobiol. A: Chem. **200**, 402–409 (2008)
5. Loving, G., Imperiali, B.: A versatile amino acid analogue of the solvatochromic fluorophore 4-*N,N*-dimethylamino-1,8-naphthalimide: a powerful tool for the study of dynamic protein interactions. J. Am. Chem. Soc. **130**, 13630–13638 (2008)
6. Yuan, D., Brown, R.G., Hepworth, J.D., Alexiou, M.S., Tyman, J.H.P.: The synthesis and fluorescence of novel *N*-substituted-1,8-naphthylimides. J. Heterocyclic Chem. **45**, 397–404 (2008)
7. Mitchell, K.A., Brown, R.G., Yuan, D., Chang, S.C., Utecht, R.E., Lewis, D.E.: A fluorescent sensor for Cu^{2+} at the sub-ppm level. J. Photochem. Photobiol. A: Chem. **115**, 157–161 (1998)
8. Bojinov, V.B., Georgiev, N.I., Bosch, P.: Design and synthesis of highly photostable yellow–green emitting 1,8-naphthalimides as fluorescent sensors for metal cations and protons. J. Fluorescence **19**, 127–139 (2009)
9. Bojinov, V.B., Panova, I.P., Chovelon, J.-M.: Novel blue emitting tetra- and pentamethylpiperidin-4-yloxy-1,8-naphthalimides as photoinduced electron transfer based sensors for transition metal ions and protons. Sens. Actuators B: Chem. **135**, 172–180 (2008)
10. Gunnlaugsson, T., Kruger, P.E., Jensen, P., Pfeffer, F.M., Hussey, G.M.: Simple naphthalimide based anion sensors: deprotonation induced colour changes and CO_2 fixation. Tetrahedron Lett. **44**, 8909–8913 (2003)
11. Veale, E.B., Gunnlaugsson, T.: Bidirectional photoinduced electron-transfer quenching is observed in 4-amino-1,8-naphthalimide-based fluorescent anion sensors. J. Org. Chem. **73**, 8073–8076 (2008)
12. Gunnlaugsson, T., McCoy, C.P., Morrow, R.J., Phelan, C., Stomeo, F.: Towards the development of controllable and reversible 'on-off' luminescence switching in soft-matter; synthesis and spectroscopic investigation of 1,8-naphthalimide-based PET (photoinduced electron transfer) chemosensors for pH in water-permeable hydrogels. Arkivoc **2003**, 216–228 (2003)
13. Ferreira, R., Remon, P., Pischel, U.: Multivalued logic with a tristable fluorescent switch. J. Phys. Chem. C **113**, 5805–5811 (2009)
14. Greenfield, S.R., Svec, W.A., Gosztola, D., Wasielewski, M.R.: Multistep photochemical charge separation in rod-like molecules based on aromatic imides and diimides. J. Am. Chem. Soc. **118**, 6767–6777 (1996)
15. Silva, A.P., Rice, T.E.: A small supramolecular system which emulates the unidirectional, path-selective photoinduced electron transfer (PET) of the bacterial photosynthetic reaction centre (PRC). Chem. Commun. 163–164 (1999)
16. Weiss, E.A., Sinks, L.E., Lukas, A.S., Chernick, E.T., Ratner, M.A., Wasielewski, M.R.: Influence of energetics and electronic coupling on through-bond and through-space electron transfer within U-shaped donor-bridge-acceptor arrays. J. Phys. Chem. B **108**, 10309–10316 (2004)
17. Li, C., Du, P., Tian, H., Erk, P.: Novel thermochromic copolymers with two luminescent colors. Chem. Lett. **32**, 570–571 (2003)
18. Niu, C.-G., Zeng, G.-M., Chen, L.-X., Shen, G.-L., Yu, R.-Q.: Proton "off-on" behaviour of methylpiperazinyl derivative of naphthalimide: a pH sensor based on fluorescence enhancement. Analyst **129**, 20–24 (2004)
19. Qu, D.-H., Wang, Q.-C., Tian, H.: A half adder based on a photochemically driven [2]rotaxane. Angew. Chem., Int. Ed. **44**, 5296–5299 (2005)
20. Qu, D.-H., Wang, Q.-C., Ma, X., Tian, H.: A [3]rotaxane with three stable states that responds to multiple-inputs and displays dual fluorescence addresses. Chem. Eur. J. **11**, 5929–5937 (2005)
21. Ruf, A., Murcia, G., Schulz, G.E.: Inhibitor and NAD^{+} binding to poly(ADP-ribose) polymerase as derived from crystal structures and homology modeling. Biochemistry **37**, 3893–3900 (1998)
22. Ryan, G.J., Quinn, S., Gunnlaugsson, T.: Highly effective DNA photocleavage by novel "rigid" Ru(bpy)3–4-nitro- and -4-amino-1,8-naphthalimide conjugates. Inorg. Chem. **47**, 401–403 (2008)
23. Quaquebeke, E.V., Mahieu, T., Dumont, P., Dewelle, J., Ribaucour, F., Simon, G., Sauvage, S., Gaussin, J.-F., Tuti, J., Yazidi, M.E., Vynckt, F.V., Mijatovic, T., Lefranc, F., Darro, F., Kiss, R.: 2,2,2-Trichloro-*N*-({2-[2-(dimethylamino)ethyl]-1,3-dioxo-2,3-dihydro-1*H*-benzo[de]isoquinolin-5-yl}carbamoyl)acetamide (UNBS3157), a novel nonhematotoxic naphthalimide derivative with potent antitumor activity. J. Med. Chem. **50**, 4122–4134 (2007)
24. Stewart, W.W.: Lucifer dyes—highly fluorescent dyes for biological tracing. Nature **292**, 17–21 (1981)
25. Middleton, R.W., Parrick, J.: Preparation of 1,8-naphthalimides as candidate fluorescent probes of hypoxic cells. J. Heterocyclic Chem. **22**, 1567–1572 (1985)
26. Lacivita, E., Leopoldo, M., Masotti, A.C., Inglese, C., Berardi, F., Perrone, R., Ganguly, S., Jafurulla, M., Chattopadhyay, A.: Synthesis and characterization of environment-sensitive fluorescent ligands for human $5\text{-}HT_{1A}$ receptors with 1-arylpiperazine structure. J. Med. Chem. **52**, 7892–7896 (2009)
27. Chang, S.C., Archer, B.J., Utecht, R.E., Lewis, D.E., Judy, M.M., Matthews, J.L.: 4-Alkylamino-3-bromo-*N*-alkyl-1, 8-naphthalimides: new photochemically activatable antiviral compounds. Bioorg. Med. Chem. Lett. **3**, 555–556 (1993)
28. Chanh, T.C., Lewis, D.E., Judy, M.M., Sogandaresbernal, F., Michalek, G.R., Utecht, R.E., Skiles, H., Chang, S.C., Matthews, J.L.: Inhibition of retrovirus-induced syncytium formation by photoproducts of a brominated 1,8-naphthalimide compound. Antiviral Res. **25**, 133–146 (1994)
29. Zhang, J., Woods, R.J., Brown, P.B., Lee, K.D., Kane, R.R.: Synthesis and photochemical protein crosslinking studies of hydrophilic naphthalimides. Bioorg. Med. Chem. Lett. **12**, 853–856 (2002)
30. Szejtli, J.: Cyclodextrins and Their Inclusion Complexes. Akademiai Kiado, Budapest (1982)
31. Atwood, J.L., Davies, J.E.D., Macnicol, D.D., Vogtle, F. (eds.): Comprehensive Supramolecular Chemistry, Volume 3: Cyclodextrins. Pergamon, Oxford, UK (1996)
32. Szejtli, J.: Introduction and general overview of cyclodextrin chemistry. Chem. Rev. **98**, 1743–1754 (1998)
33. Steed J.W., Atwood, J.L.: Supramolecular Chemistry, 2nd edn. Wiley, UK, chapter 6 (2009)
34. Nepogodiev, S.A., Stoddart, J.F.: Cyclodextrin-based catenanes and rotaxanes. Chem. Rev. **98**, 1959–1976 (1998)
35. Brochsztain, S., Rodrigues, M.A., Politi, M.J.: Inclusion complexes of naphthalimide derivatives with cyclodextrins. J. Photochem. Photobiol. A: Chem. **107**, 195–200 (1997)
36. Brochsztain, S., Politi, M.J.: Solubilization of 1,4,5,8-naphthalenediimides and 1,8-naphthalimides through the formation of novel host-guest complexes with α-cyclodextrin. Langmuir **15**, 4486–4494 (1999)
37. Campos, I.B., Brochsztain, S.: Inclusion complexes of cyclodextrins with 4-amino-1,8-naphthalimides. J. Incl. Phenom. **44**, 207–211 (2002)
38. Marcon, R.O., Brochsztain, S.: Characterization of self-assembled thin films of zirconium phosphonate/aromatic diimides. Thin Solid Films **492**, 30–34 (2005)
39. Marcon, R.O., Santos, J.G., Figueiredo, K.M., Brochsztain, S.: Characterization of a novel water-soluble 3,4,9,10-perylenetetracarboxylic diimide in solution and in self-assembled zirconium phosphonate thin films. Langmuir **22**, 1680–1687 (2006)

40. Ford, W.E.: Photochemistry of 3,4,9,10-perylenetetracarboxylic dianhydride dyes: visible absorption and fluorescence of the di(glycil)imide derivative monomer and dimer in basic aqueous solutions. J. Photochem. **37**, 189–204 (1987)
41. Douhal, A. (ed.): Cyclodextrin Materials Photochemistry, Photophysics and Photobiology, 1st edn. Elsevier, Amsterdam (2006)
42. Connors, K.A.: Binding Constants: The Measurement of Molecular Complex Stability. Wiley, New York (1987), chapter 12
43. Hoshino, M., Imamura, M., Ikehara, K., Hama, Y.: Fluorescence enhancement of benzene derivatives by forming inclusion complexes with beta-cyclodextrin in aqueous solutions. J. Phys. Chem. **85**, 1820–1823 (1981)